Inhaled Multiwalled Carbon Nanotubes Potentiate Airway Fibrosis in Murine Allergic Asthma

Jessica P. Ryman-Rasmussen[1,2], Earl W. Tewksbury[2], Owen R. Moss[2], Mark F. Cesta[1,2,3], Brian A. Wong[2], and James C. Bonner[1,2]

[1]Department of Environmental and Molecular Toxicology, North Carolina State University, Raleigh, North Carolina; [2]The Hamner Institutes for Health Sciences, Research Triangle Park, North Carolina; and [3]Cellular and Molecular Pathology Branch, National Institute of Environmental Health Sciences, Research Triangle Park, North Carolina

Carbon nanotubes are gaining increasing attention due to possible health risks from occupational or environmental exposures. This study tested the hypothesis that inhaled multiwalled carbon nanotubes (MWCNT) would increase airway fibrosis in mice with allergic asthma. Normal and ovalbumin-sensitized mice were exposed to a MWCNT aerosol (100 mg/m^3) or saline aerosol for 6 hours. Lung injury, inflammation, and fibrosis were examined by histopathology, clinical chemistry, ELISA, or RT-PCR for cytokines/chemokines, growth factors, and collagen at 1 and 14 days after inhalation. Inhaled MWCNT were distributed throughout the lung and found in macrophages by light microscopy, but were also evident in epithelial cells by electron microscopy. Quantitative morphometry showed significant airway fibrosis at 14 days in mice that received a combination of ovalbumin and MWCNT, but not in mice that received ovalbumin or MWCNT only. Ovalbumin-sensitized mice that did not inhale MWCNT had elevated levels IL-13 and transforming growth factor (TGF)-β1 in lung lavage fluid, but not platelet-derived growth factor (PDGF)-AA. In contrast, unsensitized mice that inhaled MWCNT had elevated PDGF-AA, but not increased levels of TGF-β1 and IL-13. This suggested that airway fibrosis resulting from combined ovalbumin sensitization and MWCNT inhalation requires PDGF, a potent fibroblast mitogen, and TGF-β1, which stimulates collagen production. Combined ovalbumin sensitization and MWCNT inhalation also synergistically increased IL-5 mRNA levels, which could further contribute to airway fibrosis. These data indicate that inhaled MWCNT require pre-existing inflammation to cause airway fibrosis. Our findings suggest that individuals with pre-existing allergic inflammation may be susceptible to airway fibrosis from inhaled MWCNT.

Keywords: carbon nanotubes; asthma; fibrosis; lung

CLINICAL RELEVANCE

This research has important implications for understanding the health risks of inhaled carbon nanotubes. The findings suggest that individuals with allergic asthma are most susceptible to airway remodeling caused by carbon nanotube exposure.

Carbon nanotubes (CNT) possess unique characteristics that make them highly desirable for applications in electronics, structural engineering, and medicine due to impressive electrical conductivity, mechanical strength, and ability to be derivatized for custom applications such as drug delivery (1). Given the enormous industrial demand for carbon nanotubes (the global market is predicted to grow to between $1 billion and $2 billion by 2014), there is growing concern that the development and use of engineered CNT might be accompanied by health risks caused by occupational or environmental exposures (1, 2). Structurally, CNT can be described as graphite sheets rolled into cylinders that are one ("single-walled," SWCNT) or several ("multiwalled," MWCNT) layers thick. CNT range from one to several nanometers in width and up to several microns in length. This large length to width (aspect) ratio, a property shared with asbestos fibers, has led to concern that inhaled CNT may cause asbestos-like injuries, such as pulmonary fibrosis and lung cancer (2).

A number of studies over the past 5 years have shown that liquid suspensions of CNT cause pulmonary inflammation and fibrosis when administered to the lung by intratracheal instillation or pharyngeal aspiration. These studies show that CNT, which aggregate into micron-sized bundles in aqueous media, stimulate the formation of inflammatory foci known as granulomas and fibrotic reactions within the lung parenchyma. Pulmonary fibrosis and/or granulomas have been reported in mice or rats within days after intratracheal instillation of SWCNT (3–6) or MWCNT (7). Moreover, SWCNT delivered to the lung by instillation increases production of platelet-derived growth factor (PDGF) and transforming growth factor (TGF)-β1, two growth factors that mediate the pathogenesis of fibrosis (4, 6). Granulomas are associated with large CNT aggregates in the lung that are easily visible by light microscopy, while interstitial pulmonary fibrosis appears to be associated with dispersed CNT that are detected by electron microscopy (4). A recent study showed that SWCNT dispersed with organic solvents to disrupt Van der Waals forces resulted in less deposition in the large airways but more in the interstitium, where the fibrotic response was significantly increased (8). While instillation or aspiration experiments demonstrate that CNT are fibrogenic, these methods do not accurately model deposition patterns of CNT, and much emphasis has been placed on the need for inhalation studies.

There is recent evidence from whole-body inhalation studies in rodents that the method of pulmonary administration of MWCNT affects deposition patterns and pathology. A study that compared instillation with inhalation indicated that MWCNT inhaled by mice showed a more diffuse pattern of deposition with less severe pathologic lesions than those that were observed after intratracheal instillation of a bolus dose (9). Another recent study showed that inhaled MWCNT did not cause lung inflammation or fibrosis in rats, but did cause systemic immunosuppression and spleenic oxidative stress (10). This result greatly differed from earlier work that showed MWCNT administered by intratracheal instillation resulted in pulmonary inflammation and

(*Received in original form July 22, 2008 and in final form September 1, 2008*)

This study was funded by The American Chemistry Council's Long Range Research Initiative provided to The Hamner Institutes for Health Sciences, The Intramural Research Program of the National Institutes of Health, National Institute of the Environmental Health Sciences, and North Carolina State University's College of Agricultural and Life Sciences.

Correspondence and requests for reprints should be addressed to James C. Bonner, Ph.D., North Carolina State University, Box 7633, Raleigh, NC 27695. E-mail: james_bonner@ncsu.edu

Am J Respir Cell Mol Biol Vol 40. pp 349–358, 2009
Originally Published in Press as DOI: 10.1165/rcmb.2008-0276OC on September 11, 2008
Internet address: www.atsjournals.org

fibrosis (7). Therefore, it appears that MWCNT cause little inflammation or fibrosis when delivered by inhalation, but significant injury, inflammation, and fibrosis when administered by intratracheal or pharyngeal routes in normal lung tissue. Despite the reported lack of lung injury from inhaled MWCNT (10), it is reasonable to postulate that adverse effects of inhaled MWCNT might be manifested under conditions of pre-existing inflammation such as allergic asthma.

Asthma is a chronic inflammatory disease that afflicts millions of individuals in the United States and worldwide. The pathogenesis of asthma involves chronic remodeling of the airways of the lung, including eosinophilic inflammation, mucus hypersecretion from the airway epithelium, airway smooth muscle cell thickening, and airway fibrosis (11). Many of these pathologic features of asthma are mediated by IL-13, a cytokine that is secreted by Th2 lymphocytes in response to allergen challenge (12). In turn, IL-13 activates a variety of other pulmonary cell types to produce cytokines and growth factors that play a diversity of roles in inflammation and fibrosis. For example, we have reported that IL-13 stimulates lung fibroblasts, the primary target cell type in fibrosis, to increase the production of PDGF, a potent fibroblast mitogen (13). IL-13 has also been reported to increase the production and activation of TGF-β1, the primary growth factor that stimulates fibroblasts to produce collagen and promote scar formation (14).

Epidemiologic studies have shown a correlation between the incidence and severity of asthma attacks and levels of airborne particulates (15). Furthermore, it has been suggested that the ultrafine (or nanoscale) fraction of particulate matter is most important to the exacerbation of asthma (16). In the present study, we hypothesized that inhaled MWCNT produce greater injury and fibrosis in mice with pre-existing allergic lung inflammation. To test this hypothesis, we sensitized mice to ovalbumin allergen, a common mouse model of asthma, and then exposed the mice to a brief, high dose of MWCNT by nose-only inhalation. The results of our study suggest that individuals with asthma represent a susceptible subpopulation that could be at greater risk for the possible profibrotic effects of engineered nanomaterials.

MATERIALS AND METHODS

Animals

Pathogen-free adult male C57BL/6 mice were obtained from Charles River Laboratories (Raleigh, NC) at 6 to 8 weeks of age. Mice were randomized by weight upon receipt and divided into eight treatment groups. Animals were individually housed in polycarbonate cages with Alphi-dri cellulose bedding (Shepherd Specialty Papers, Kalamazoo, MI) in a temperature- and humidity-controlled environment with a 12-hour light/dark cycle at an International Association for Assessment and Accreditation of Laboratory Animal Care (AAALAC)-accredited facility. Mice were given food (NIH-07 ground pellets; Zeigler Brothers, Gardners, PA) and water *ad libitum* when not in inhalation chambers. Bedding and food meet National Toxicology Program (NTP) standards and are certified by the manufacturer as free of pesticides, resins, or aflotoxin. All mice were acclimated to inhalation chambers 1 week before aerosol exposure by adaptation to chambers from 1 hour to 6 hours over a 5-day period. All procedures requiring animal use were approved by the Institutional Animal Care and Use Committee (IACUC) at The Hamner Institutes.

Experimental Design

Mice ($n = 40$) were sensitized to ovalbumin (98% pure, grade V; Sigma-Aldrich, St. Louis, MO) over a 2-week period by intraperitoneal injection 14 days before inhalation exposure (−14 d) and 7 days before inhalation exposure (−7 d) with 20 μg of ovalbumin adsorbed onto 2 mg of alum (Accurate Chemical and Scientific Corporation, Westbury, NY) in 200 μl of sterile saline as previously described (17). Control mice ($n = 40$) were similarly injected with 200 μl of saline. One day before inhalation exposure (−1 d), mice were challenged intranasally with 100 μl of 1% ovalbumin in saline or saline alone while under isoflurane anesthesia. A high airborne concentration of MWCNT ($\sim$ 100 mg/m^3) was intentionally chosen to deliver an alveolar dose of MWCNT within a 6-hour period that would be in the 10 mg/kg range, which would be consistent with a previous study using intratracheally instilled MWCNT (7). On the day of inhalation exposure (0 d), sensitized and unsensitized mice were exposed to aerosolized nanotubes or saline vehicle for 6 hours in nose-only inhalation chambers and returned to the vivarium for 1 day or 14 days. One hour before killing at 1 day, mice were injected (intraperitoneally) with 50 mg/kg body weight of 5′-bromodeoxyuridine (Sigma-Aldrich). Mice were anesthetized with 90 mg/kg pentobarbital (intraperitoneally) and killed by exangunation. Lungs were lavaged with Dulbecco's Phosphate Buffered Saline (DPBS) and bronchoalveolar lavage fluids (BALFs) saved for lactate dehydrogenase (LDH), total protein, and enzyme-linked immunosorbent assay (ELISA). The middle and caudal lobes of the right lung were collected for RT-PCR and stored in RNAlater as instructed by the manufacturer (Ambion, Austin, TX) and the cranial lobe frozen at −80°C for later collagen determination. The left lung was insufflated with 10% neutral buffered formalin, fixed for 72 hours, transferred to 70% ethanol, and embedded in parafin. Five-micrometer sections were processed for histopathology with a Masson's trichrome or hematoxylin and eosin stain.

Characterization of Bulk CNT

MWCNT of "standard" length (0.5–40 μm) synthesized by carbon vapor deposition (CVD) with nickel and lanthanum catalysts were purchased from Helix Material Solutions, Inc. (Richardson, TX). Characterization of the size, purity, and elemental composition of the MWCNT was provided by Helix, Inc. We verified these parameters by independent analysis (Millenium Research Laboratories Inc., Woburn, MA). The characterizations of bulk MWCNT provided by the manufacturer and independently are summarized in Table 1. Size was characterized by transmission electron microscopy (TEM) and scanning electron microscopy (SEM). Purity was determined by thermogravimetric analysis (TGA). Elemental analysis was performed by energy dispersive X-ray analysis (EDX) and inductively coupled plasma Auger electron spectroscopy (ICP-AES). EDX data were expressed as the average and SEM of three different spots for each element. The EDX data provided by both groups were in agreement for carbon, which was present at approximately 94%. Composition data for oxygen, nickel, and lanthanum differed between the two groups, which is not surprising, given the lower abundance of these elements coupled with the high variability in this technique as a result of spot measurements on a nonhomogenous sample. The manufacturer found more oxygen by this method than the contractor (6.4% versus 0.71 ± 0.19%), but less nickel (0.12% versus 5.53 ± 3.92%). The contractor did not detect lanthanum, but the manufacturer did find it present at 0.06%. The contractor also measured elemental composition by ICP-AES. Lanthanum was observed at 0.03%. Nickel values were lower than those observed by EDX, at 0.34%. Oxygen values were consistent with EDX data, and carbon content was slightly greater at 99.00%. The specific surface area was determined by Brunauer-Emmett-Teller method (BET) and reported by the manufacturer as 40 to 300 m^2/g. This was consistent with independent testing at 109.29 m^2/g. Purity was assessed by TGA. TGA provided by the manufacturer described MWCNT as more than 95% pure, which was in agreement with greater than 94% as determined by the contractor. The manufacturer also observed less than 2% amorphous carbon and less than 0.2% residual ash. Size was assessed by SEM (Figure 1A) and TEM (Figure 1B). The manufacturer's description of MWCNT as being 10 to 30 nm average external diameter was slightly less than the contractor's values of 30 to 50 nm. The 0.5 to 40 μm average length was consistent with the 0.3 to 50 μm values obtained independently.

MWCNT Aerosol Generation and Characterization

Autoclaved MWCNT were dry-milled in a Retsch Mixer Mill (Retsch Inc., Newtown, PA) for 5 minutes at 30 cycles per second. The milled MWCNT were suspended in a sterile, biocompatible nonionic surfactant,

TABLE 1. COMPARISON OF PHYSICOCHEMICAL CHARACTERIZATION OF BULK MULTIWALLED CARBON NANOTUBES BY THE MANUFACTURER AND AN INDEPENDENT CONTRACT LABORATORY

	Manufacturer (Helix)	Independent (MRL)
Purity (TGA)	>95%	>94%
Amorphous Carbon (TGA)	<2%	ND
Ash (TGA)	<0.2 wt %	ND
C (EDX)	93.4%	93.75 ± 3.93%
O (EDX)	6.4%	0.71 ± 0.19%
Ni (EDX)	0.12%	5.53 ± 3.92%
La (EDX)	0.06%	ND
C (ICP-AES)	ND	99.00%
O (ICP-AES)	ND	0.63%
Ni (ICP-AES)	ND	0.34%
La (ICP-AES)	ND	0.03%
Avg. Diameter (TEM)	10–30 nm	30–50 nm
Length (TEM, SEM)	0.5–40 μm	0.3–50 μm
BET Surface Area	40–300 m^2/g	109.29 m^2/g

Definition of abbreviations: BET, Brunauer-Emmett-Teller method; EDX, energy dispersive X-ray analysis; ICP-AES, inductively coupled plasma Auger electron spectroscopy; MRL, Millennium Research Laboratories, Inc.; ND, not determined; SEM, scanning electron microscopy; TEM, transmission electron microscopy; TGA, thermogravimetric analysis.

1% pluronic F-68 (Sigma-Aldrich) in sterile DPBS. The MWCNT suspensions were further diluted with DPBS to achieve the desired final concentration of approximately 5 mg/ml MWCNT in 0.1% pluronic F-68. Aerosols of MWCNT suspensions or the DPBS/0.1% pluronic F-68 vehicle were generated with a 6-Jet Collision nebulizer (Model CN-25; BGI, Inc., Waltham, MA) with compressed, hepa-filtered air (~ 21 psi) used as the carrier gas. Nebulized aerosols were passed through a trap (Model F73G-3AN-QT3; Norgren, Littleton, CO) to remove any large droplets, followed by a ^{85}Kr source (BGI-085, 10 mCi nomial; Isotope Products, Valencia, CA) and a silica gel dryer (Model 3062; TSI, Inc., St. Paul, MN) to remove water. Ten animals were exposed to the aerosols on a Cannon nose-only tower (Lab Products, Maywood, NJ) for a 6-hour period at a flow rate of approximately 217 ml/minute per port. The pressure at the tower was monitored with a Magnehelic pressure gauge (Magnehelic; Dwyer Instruments, Inc., Michigan City, IN) and maintained near 0.0 inches of water. An Aerodynamic Particle Sizer (APS, Model 3321; TSI) and a Scanning Mobility Particle Sizer (SMPS, Model 3934; TSI) were used to monitor the particle size at the inlet of the tower during each exposure. Data merge software (Model 390069; TSI) was used to combine APS and SMPS size distributions. TEM and SEM samples of the MWCNT aerosol were captured from a tower port using an electrostatic precipitator (ESP; Intox Products, Moriarty, NM). Aerosol mass concentration was determined gravimetrically for each exposure at a tower port using 25-mm glass fiber filters (G15WP02500; Osmonics, Inc., Minnetonka, MN).

Estimation of CNT Delivered Dose to Lung Tissues

We estimate an alveolar deposition dose of approximately 12 mg/kg and a tracheobronchial deposition dose of 4 mg/kg. Assuming that an adult C57BL/6 mouse with an average body mass (M) of 24 g has a respiratory minute volume (RMV) of 0.0273 L/minute (2) and that the alveolar deposition fraction (DF) is approximately 30% particles of with an MMAD of 714 ± 328 nm (and the tracheobronchial deposition is ~ 10%) (18) at a time (T) of 6 hours, the doses at 100 mg/m^3 concentration (C) can be calculated according to the formula (6):

$$\text{Dose} = (\text{RMV} \times \text{DF} \times \text{T} \times \text{C})/\text{M}.$$

At an RMV of 0.0273 L/minute, the aerosol flow rate of 0.217 L/minute was more than sufficient to prevent dose dilution by mixing of expired air with the aerosol.

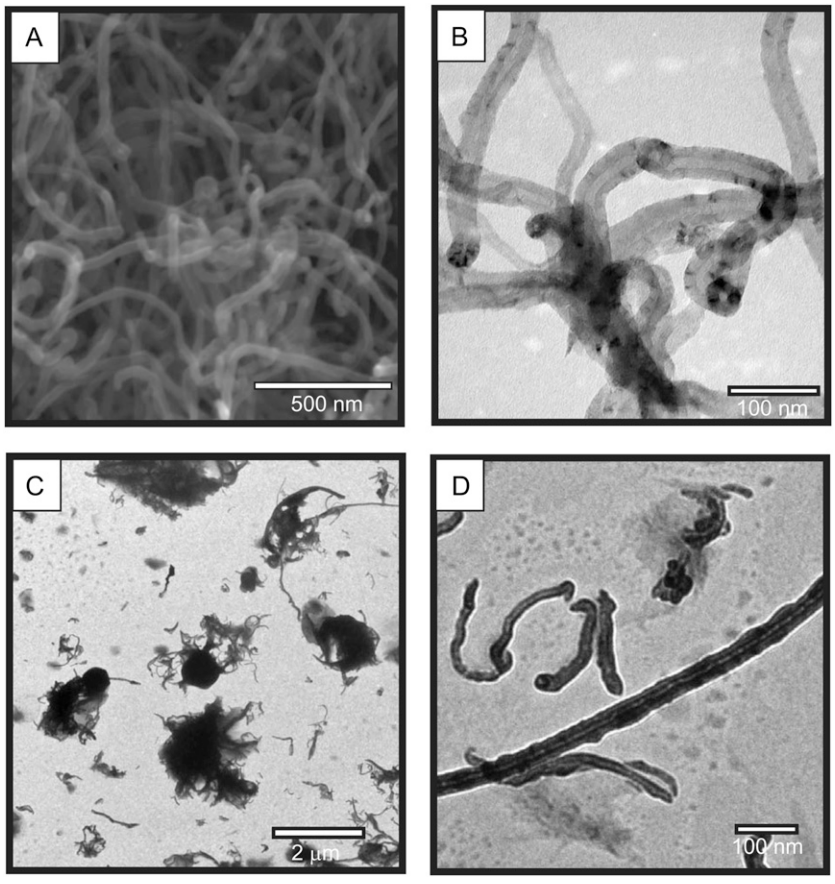

Figure 1. Photomicrographs of multiwalled carbon nanotubes (MWCNT) before and after aerosolization. (*A*) SEM of bulk nanotubes. (*B*) Transmission electron microscopy (TEM) of bulk nanotubes. (*C* and *D*) TEM photomicrographs of nanotubes collected from filters after 6 hours of inhalation. *Scale bars*: *A*, *B*, and *D*, 100 nm; *C*, 2,000 nm.

Bronchoalveolar Lavage, Clinical Chemistry, and Cytology

Lungs were serially lavaged five times with 1.0 ml DPBS. Lavages 1–2 and 3–5 were combined and cells recovered by centrifugation. An aliquot of the combined lavage 1–2 supernatant (the bronchoalveolar lavage fluid, or BALF) was taken for LDH (LD Liquid Reagent; Pointe Scientific, Canton, MI) and total protein (Coomassie Plus Protein Assay Reagent; Pierce, Rockford, IL) assays with a COBAS FARA II automated analyzer (Roche Diagnostic Systems Inc., Montclair, NJ) and the remainder stored at −80°C for ELISA assays. The cell pellets from all five lavages were resuspended in Ham's F12 medium with 10% FBS and counted using a Coulter counter (Beckman-Coulter, Marietta, GA). A Shandon Cytospin (Fisher Scientific, Pittsburgh, PA) was used to plate 50,000 cells per animal on glass slides, followed by fixation and staining with the Hema 3 Stain Set (Fisher Scientific). Differential cell counts were then performed on at least 200 cells per sample.

Sircol Assay for Soluble Collagen

The right cranial lobe of each mouse lung was suspended in DPBS at 50 to 100 mg tissue per ml and homogenized for 60 seconds with a Tissuemiser homogenizer (Fisher Scientific). Triton X-100 was added to 1% and the samples incubated for 18 hours at room temperature. Acetic acid was added to each sample to a final concentration of 0.5 M and incubated at room temperature for 90 minutes. Cellular debris was pelleted by centrifugation and the supernatant analyzed for total protein with the BCA Assay kit (Pierce/ThermoFisher Scientific) according to manufacturer's instructions. The Sircol Soluble Collagen Assay kit (Biocolor Ltd., Carrickfergus, UK) was used to extract collagen from duplicate samples by using 200 μl of supernatant and 800 μl of Sircol Dye Reagent according to the manufacturer's instructions. Similarly prepared collagen standards (10–50 μg) were run in parallel. Collagen pellets were washed twice with denatured alcohol and dried before suspension in Alkali reagent. Absorbance at 540 nm was read on a Multiskan EX microplate spectrophotometer (Fisher Scientific) microplate reader with Ascent software. Data were expressed as μg of soluble collagen per mg of total protein.

ELISA

Quantikine ELISA kits (R&D Systems, Minneapolis, MN) were used to assay BALF for total TGF-β1 (active and inactive forms), IL-13, MCP-1/JE, eotaxin, and PDGF-AA 1 day after inhalation. Duplicate samples using 50 μl BALF were used for each animal. Assays were performed as per kit instructions and absorbances read on a Multiskan EX microplate spectrophotometer microplate reader (ThermoFisher Scientific). Values were normalized relative to total protein in BALF and were expressed as mean ± SEM.

Quantitative Morphometry

Quantification of the thickness of collagen surrounding bronchioles was performed according to a previously published procedure developed in our laboratory (19, 20). Briefly, photomicrographs of trichrome-stained sections were digitized and the thickness of the collagen layer surrounding the bronchioles measured at eight equidistant points and averaged. Five airways per animal were analyzed in a random, blinded manner, and the data were expressed as the mean ± SEM of five animals per treatment group per time point.

Electron Microscopy

Lung tissues were post-fixed in 1% osmium tetroxide in 0.1 M sodium phosphate buffer, pH 7.2, dehydrated through graded ethanol solutions, cleared in acetone, and then infiltrated and embedded in Spurr's resin. Unstained thin sections (800–1,000 μm) were mounted on copper grids and then examined on a Philips EM208S transmission electron microscope.

RT-PCR

Two-step, TaqMan quantitative RT-PCR was used to quantify expression of genes of interest in lung tissue 1 day after inhalation. Total RNA was extracted from the right cranial and caudal lobes of each lung using an RNEasy Mini Kit (Qiagen, Valencia, CA) and converted to cDNA with the High Capacity cDNA Archive Kit (Applied Biosystems, Foster City, CA). RT-PCR was performed on an ABI PRISM 7000 using 50 to 100 ng of cDNA per reaction, TaqMan Universal PCR Master Mix, and TaqMan Gene Expression Assays for TGF-β1 (Mm03024053_m1), IL-5 (Mm00439646_m1), IL-13 (Mm00434204_m1), MCP-1/JE/CCL2 (Mm00441242_m1), eotaxin/CCL11 (Mm00441238_m1), CXCL9/MIG (Mm0043946_m1), CXCL10/IP-10 (Mm00445235_m1), PDGF-A (Mm00833533_m1), PDGF-Rα (Mm00440701_m1), pro-collagen type 1, α2 (Col1A2, Mm00483888_m1), and connective tissue growth factor (CTGF, Mm00525790_g1). The comparative C_T method was used to quantify message relative to a eukaryotic 18S ribosomal RNA (Hs99999901_s1) external sample. Each reaction was performed in duplicate and data expressed as mean ± SEM.

Data and Statistical Analysis

All graphs were constructed and statistical analysis performed using GraphPad Prism software v. 5.00 (GraphPad Software, Inc., San Diego, CA). A one-way ANOVA with a *post hoc* Tukey or Bonferroni test was used to identify significant differences among treatment groups. In some cases, a Kruskal-Wallace nonparametric ANOVA with a *post hoc* Dunn's test was used. Significance was set at $P < 0.05$ unless otherwise stated.

RESULTS

Aerosolized MWCNT Are Inhaled as a Mixture of Aggregated and Free Nanotubes

TEM and SEM clearly identified our commercial product as high purity MWCNT (Figures 1A and 1B). Next, it was important to show that we were aerosolizing the MWCNT and to define particle size and aggregation status. Particle size characterizations showed the aerosol had an average mass median aerodynamic diameter (MMAD ± SD) of 714 ± 328 nm with a geometric standard deviation of approximately 2. The particle number size distribution (± SD) was 160 ± 38.9 nm. The MWCNT aerosol deposited on collection filters during animal dosing was also characterized by TEM (Figures 1C and 1D). The average concentration of MWCNT in the aerosol (± SD) was 103 ± 8.34 mg/m^3. MWCNT appeared as amorphous aggregates 2 μm in diameter or less with protruding tubes extending beyond the nexus. Smaller aggregates and individual MWCNT were also present (Figure 1C). Individual MWCNT resolved at higher magnification (Figure 1D) confirmed the identity as equivalent to the bulk material (Figure 1B).

Inhaled MWCNT Do Not Cause an Increase in LDH Release or Total Lung Protein

No differences in LDH release, a measure of cytotoxicity, were observed in BALF among the treatment groups 1 day after inhalation, and MWCNT-treated animals showed a significant decrease in LDH release compared with controls 14 days after exposure (data not shown). LDH levels for unsensitized, MWCNT-treated mice (0.72 ± 0.06 U/mg total protein) were significantly less than controls (1.04 ± 0.12 U/mg). Similarly, LDH levels for ovalbumin-sensitized MWCNT-treated mice (0.65 ± 0.09 U/mg) were less than for saline-treated controls (0.97 ± 0.10 U/mg). No differences in total protein were observed at 1 day or at 14 days (data not shown).

Inhaled MWCNT Are Evenly Distributed in the Lung and Engulfed by Macrophages

Gross observations revealed that inhaled MWCNT were homogeneously distributed in the mouse lung (Figure 2A). In both sensitized and normal mice, histopathology showed some MWCNT agglomerates on the surfaces of alveolar ducts and

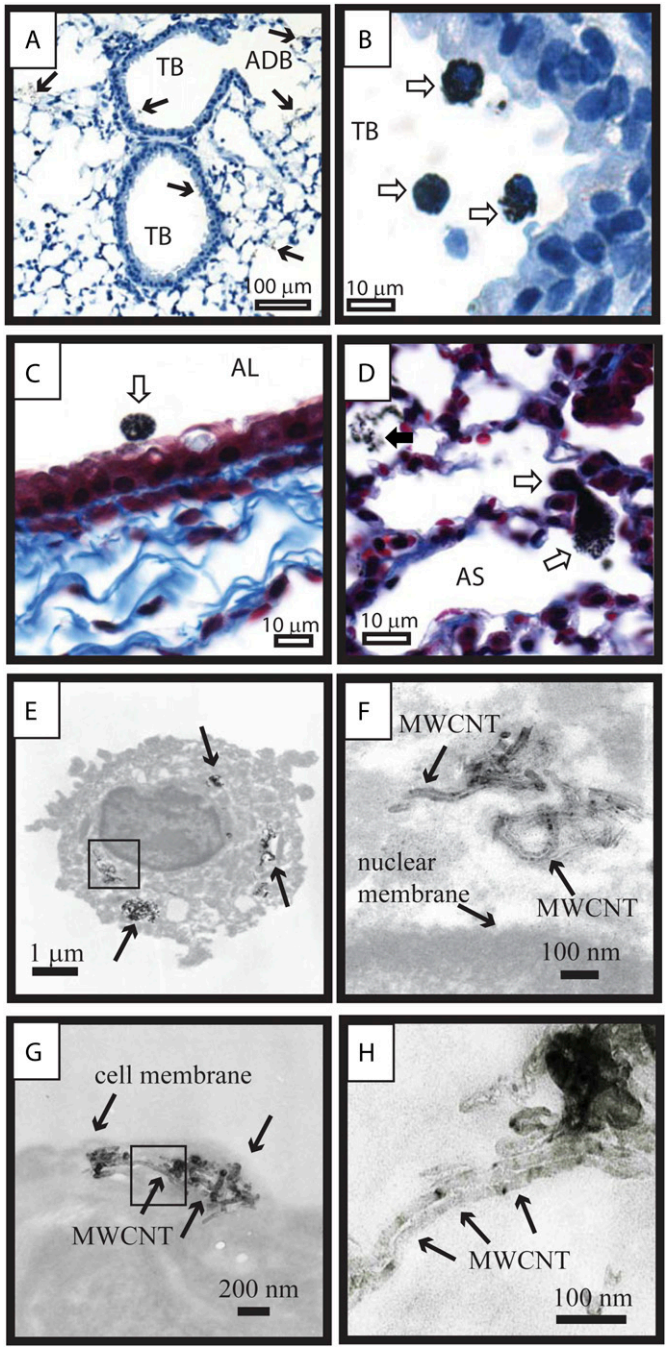

Figure 2. MWCNT distribution in lung tissue 1 day after inhalation exposure. (*A*) Low magnification (×20) of lung from a mouse exposed to MWCNT after 1 day. MWCNT aggregates deposited at alveolar duct bifurcation (ADB), terminal bronchioles (TB), and on alveolar surfaces as indicated by *arrows* (hematoxylin stain). (*B*) Light micrograph showing MWCNT in macrophages in a terminal bronchiole (TB) indicated by *open arrows* (hematoxylin stain). (*C*) Light micrograph showing MWCNT-positive alveolar macrophage (*open arrow*) on the bronchiolar epithelium in the lung of an ovalbumin-challenged mouse (Masson's trichrome stain). (*D*) Agglomerated MWCNT (*solid arrow*) and MWCNT-laden alveolar macrophages migrating through an alveolar septa (*open arrows*) (Masson's trichrome stain). (*E*) TEM of MWCNT within an alveolar macrophage. (*F*) Higher magnification of MWCNT in *E* showing nanotube structure. (*G*) TEM of unstained lung section showing aggregrate of MWCNT beneath the cell membrane of a type I epithelial cell. (*H*) Higher magnification of MWCNT shown in *G* showing distinct nanotube structure.

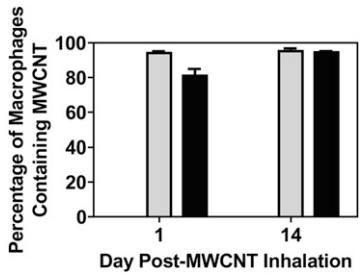

Figure 3. Persistence of MWCNT in macrophages at 1 and 14 day after inhalation exposure. Bronchoalveolar lavage (BAL) cells from cytospin were counted and the data expressed as percentage MWCNT-postive or MWCNT-negative macrophages relative to the number of total macrophages. *Shaded bars*, sal/MWCNT; *solid bars*, OVA/MWCNT.

within alveoli, indicating delivery of the aerosol to the distal airways (Figure 2A). Importantly, no airway obstruction by MWCNT was observed. By light microscopic evaluation, MWCNT were observed primarily as agglomerates in alveolar macrophages at 1 and 14 days after inhalation (Figures 2B–2D). However, TEM identified small aggregates and individual MWCNT within alveolar macrophages (Figures 2E and 2F). TEM also revealed that MWCNT were taken up by lung epithelial cells (Figures 2G and 2H). Importantly, these results showed that MWCNT maintained tube-like structure after aerosolization, inhalation, deposition, and uptake by lung cells.

Inhaled MWCNT Persist in Alveolar Macrophages within the Lung for at Least 2 Weeks

Alveolar macrophages containing MWCNT were easily identified by light microscopy and constituted the majority of total macrophages (Figure 2, Figure 3). The numbers of MWCNT-positive macrophages in BAL cytospins were counted relative to the total number of macrophages to estimate the persistence of MWCNT in the lung phagocyte population. Greater than 80% of the total number of macrophages retrieved by BAL contained MWCNT, and the relative percentage of MWCNT-positive macrophages did not decrease by 14 days after exposure, nor were there differences in the relative percentages of MWCNT-positive macrophages between unsensitized and ovalbumin-sensitized mice (Figure 3).

Inhaled MWCNT Cause Transient Neutrophilia that Is Enhanced by Ovalbumin Allergen Challenge

The results of the BALF cell differential counts are summarized in Table 2. One day after inhalation, neutrophils were significantly elevated in unsensitized animals that inhaled MWCNT compared with controls, and were also elevated for all animals sensitized with ovalbumin. There was also a trend ($P < 0.1$) for increased neutrophils in sensitized animals that inhaled MWCNT compared with unsensitized, MWCNT-inhaling animals. Neutrophil counts returned to basal levels by 14 days. Eosinophil counts for all sensitized animals were elevated at 1 day, but this elevation was not statistically significant due to large variability. Lymphocyte counts remained at basal levels for all treatment groups at both time points. The number of macrophages remained largely unchanged by all treatments.

Combined Ovalbumin Allergen Challenge and MWCNT Inhalation Cause Airway Fibrosis

At 1 day, collagen thickness around airways was similar in all dose groups, and no significant differences were found by quantitative morphometry (data not shown). At 14 days, histopathology showed an apparent increase in the thickness of collagen in the

TABLE 2. PERCENTAGES OF CELL TYPES IN BRONCHOALVEOLAR LAVAGE FLUID 1 d AND 14 d AFTER INHALATION

	Neutrophil	Lymphocyte	Eosinophil	Macrophage
Sal/sal (1 d)	0.09 ± 0.09	1.25 ± 0.83	0.00 ± 0.00	98.65 ± 0.92
Sal/sal (14 d)	0.00 ± 0.00	0.52 ± 0.24	0.28 ± 0.28	98.93 ± 0.59
Sal/MWCNT (1 d)	11.31 ± 2.21*	1.37 ± 0.38	1.21 ± 0.55	86.09 ± 2.42†
Sal/MWCNT (14 d)	0.00 ± 0.00	0.54 ± 0.16	0.00 ± 0.00	99.3 ± 0.32
OVA/sal (1 d)	11.22 ± 9.55	2.20 ± 0.98	14.48 ± 12.63	72.35 ± 16.56
OVA/sal (14 d)	0.83 ± 0.42	2.02 ± 1.12	1.37 ± 0.57	95.77 ± 2.02
OVA/MWCNT (1 d)	28.34 ± 7.91‡	2.13 ± 0.38	14.22 ± 6.56	55.30 ± 8.42§
OVA/MWCNT (14 d)	0.08 ± 0.08	2.92 ± 1.25	2.55 ± 1.67	94.45 ± 2.88

Definition of abbreviations: MWCNT, multiwalled carbon nanotubes; OVA, ovalbumin.
Data are mean ± SEM for 4 animals (sal/sal at 1 d) or 5 animals (all others).
* $P < 005$ compared with sal/sal neutrophil count at 1 d.
† $P < 005$ compared with sal/sal macrophage count at 1 d.
‡ $P < 01$ compared with sal/MWCNT neutrophil count at 1 d.
§ $P < 005$ compared with sal/MWCNT macrophage count at 1d.

reticulum around the basement membrane of the bronchioles in sensitized animals that inhaled MWCNT relative to unsensitized animals that inhaled MWCNT and sensitized and unsensitized saline-inhaling controls (Figures 4A–4D). This was confirmed by quantitative morphometry, which showed a statistically significant increase relative to unsensitized animals that inhaled MWCNT or sensitized animals that inhaled saline (Figure 4E). Also, un-sensitized animals that inhaled MWCNT did not have a significant increase in airway collagen deposition compared with saline-inhaling controls. No significant differences in soluble collagen production as measured by Sircol Assay in whole lung (right cranial lobe) were observed among any of the treatment groups 1 day and 14 days after inhalation (data not shown). Immunostaining for BrdU was also performed in animals killed at 1 day. The rapidly dividing epithelial cells along the basement membrane of the duodenum from each animal stained positive for BrdU, indicating successful BrdU uptake and detection. However, no focal areas of BrdU staining were observed in lung tissue for controls or MWCNT-treated animals.

IL-13 Levels Increased by Ovalbumin Challenge Are Not Significantly Affected by MWCNT Inhalation

IL-13 protein was quantified in the BALF by ELISA and expression of IL-13 mRNA in lung tissue was quantified by RT-PCR. One day after inhalation of saline or MWCNT, IL-13 protein levels in the BALF were not detectable by ELISA in any unsensitized animals that inhaled saline or MWCNT (threshold 7.8 pg/ml). As expected, ovalbumin challenge increased IL-13 levels, and yet the level of IL-13 detected in ovalbumin-sensitized animals was not significantly affected by MWCNT inhalation (Figure 5A). Similarly, IL-13 mRNA in lung tissue was increased by ovalbumin challenge but not different between mice that received ovalbumin or ovalbumin plus MWCNT after 1 day (Figure 5B). IL-13 mRNA and protein were not detectable in any groups at Day 14 (data not shown).

Both PDGF-AA and TGF-β1 Are Increased by the Combination of Ovalbumin Allergen Challenge and MWCNT Inhalation

A fibrogenic response requires the combined actions of PDGF to stimulate fibroblast replication and TGF-β1 to drive collagen deposition by fibroblasts. PDGF-AA levels in the BALF were significantly elevated 1 day after MWCNT inhalation in the absence or presence of ovalbumin (Figure 6A). Ovalbumin sensitization alone did not increase PDGF-AA levels in BALF. In contrast, TGF-β1 levels in BALF were increased by ovalbumin in the absence or presence of MWCNT, but MWCNT inhalation exposure alone did not increase TGF-β1 (Figure 6B). Both PDGF-AA and TGF-β1 were simultaneously increased only with combined ovalbumin sensitization and MWCNT inhalation exposure. At Day 14, no significant differences were observed for PDGF-AA or TGF-β1 protein levels (data not shown).

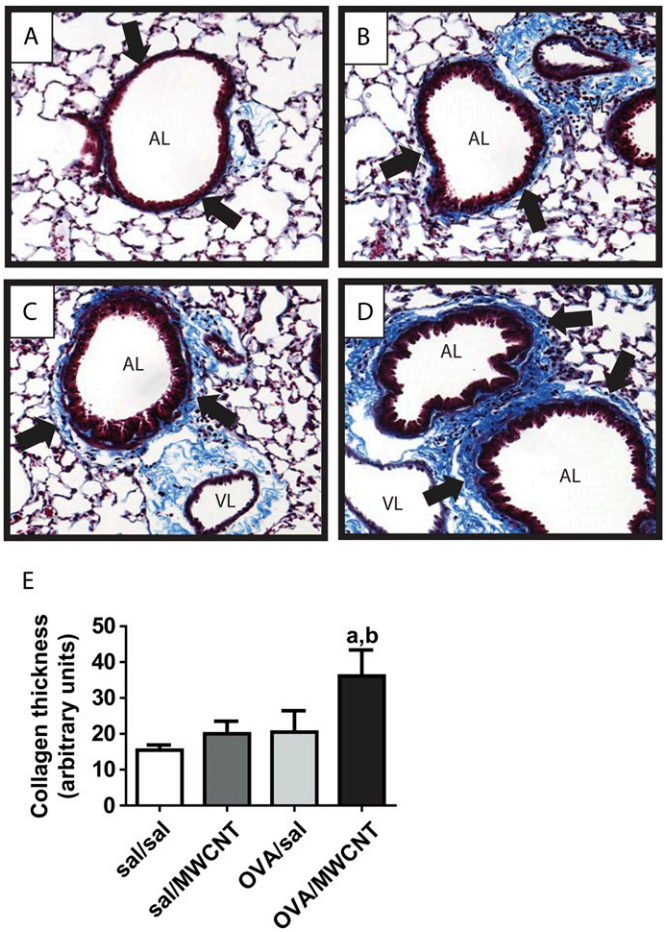

Figure 4. Masson's trichrome stain for collagen (*blue*) around airways 14 days after inhalation (*magnification*: ×20). (*A*) Unsensitized, saline inhalation. (*B*) Ovalbumin-sensitized, saline inhalation. (*C*) Unsensitized, MWCNT inhalation. (*D*) Ovalbumin-sensitized, MWCNT inhalation. (*E*) Quantitative morphometry for collagen deposition around airways at 14 days. $^{a}P < 0.01$ compared with sal/MWCNT; $^{b}P < 0.01$ compared with OVA/sal. Data are the mean ± SEM of five (sal/sal) or seven animals (all others).

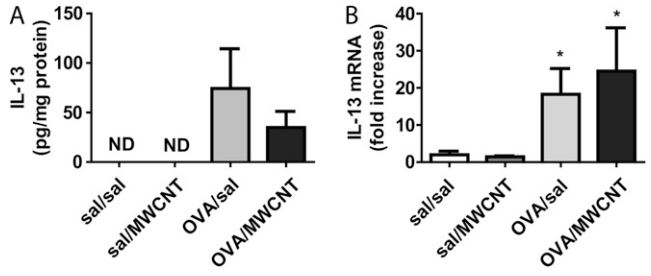

Figure 5. IL-13 mRNA and protein levels at 1 day after inhalation of MWCNT. (*A*) IL-13 in BAL fluid (BALF) was measured by enzyme-linked immunosorbent assay (ELISA). No IL-13 was detected in mice that did not receive ovalbumin challenge (ND, not detectable), nor was IL-13 detected in any groups at 14 days (not shown). (*B*) IL-13 mRNA levels measured by Taqman quantitative real-time RT-PCR. $*P < 0.05$ compared with sal/sal control group.

IL-5 mRNA Is Synergistically Increased by the Combination of Ovalbumin Sensitization and MWCNT Inhalation Exposure

IL-5 mRNA levels in whole lung tissue measured by RT-PCR were synergistically increased by combined ovalbumin challenge and MWCNT exposure, yet neither ovalbumin nor MWCNT alone increased IL-5 mRNA levels above the saline control (Figure 7A). We also evaluated mRNA levels for several chemokines (MCP-1, eotaxin, and CXCL9). MCP-1 mRNA levels were significantly increased by MWCNT exposure in the absence or presence of ovalbumin sensitization (Figure 7B). Eotaxin mRNA levels were also increased by MWCNT, but also by ovalbumin (Figure 7C). mRNA levels for CXCL9, an interferon-inducible chemokine, were increased by ovalbumin but not by MWCNT (Figure 7D). The mRNA levels for all of these cytokine/chemokine returned to basal expression levels by Day 14, with no differences between exposure groups (data not shown).

DISCUSSION

The present study was designed to test the hypothesis that inhaled MWCNT would cause greater lung injury and fibrosis in mice that had pre-existing allergic inflammation. We found that inhaled MWCNT caused no significant fibrosis in mice that did not receive ovalbumin challenge, nor did we observe any increase in total lung protein and LDH release into the BAL fluid from MWCNT-exposed mice. However, mice that received

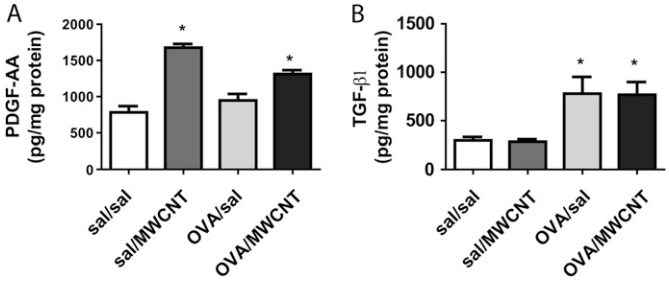

Figure 6. Levels of platelet-derived growth factor (PDGF) and transforming growth factor (TGF)-β1 protein in BALF 1 day after MWCNT inhalation. (*A*) PDGF-AA measured by ELISA. $*P < 0.05$ compared with sal/sal control group. (*B*) Total TGF-β1 measured by ELISA. $*P < 0.05$ compared with sal/sal or sal MWCNT. Data are the mean ± SEM of 9 (sal/sal) or 10 animals (all others) from samples assayed in duplicate.

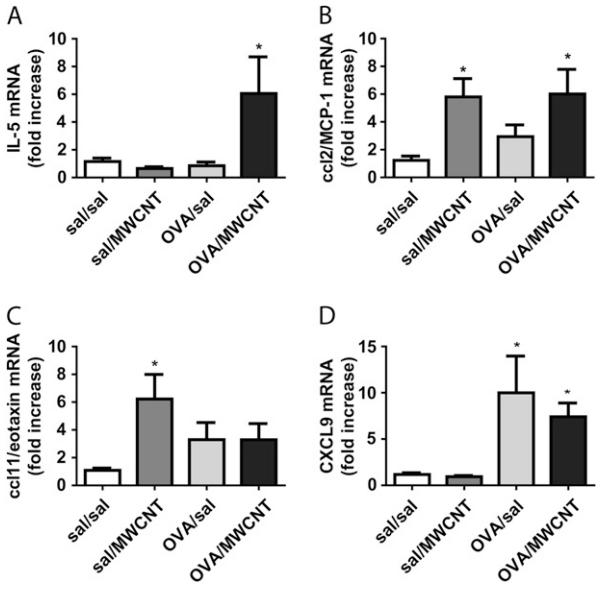

Figure 7. mRNA levels of IL-5 and chemokines in lung tissue at 1 day after inhalation exposure. Taqman quantitative real-time RT-PCR was used to measure changes in mRNA levels. (*A*) IL-5. $*P < 0.05$ compared with sal/sal. (*B*) CCL2/MCP-1. $*P < 0.05$ compared with sal/sal control group. (*C*) CCL11/eotaxin. $*P < 0.05$ compared with sal/sal. (*D*) CXCL9. $*P < 0.05$ compared with sal/sal. Data are the mean ± SEM of 9 (sal/sal) or 10 animals (all others) from samples assayed in duplicate.

ovalbumin challenge before MWCNT inhalation exposure developed significant airway fibrosis as determined by quantitative morphometry. Some neutrophilic inflammation was observed in the lungs of mice that inhaled MWCNT, but this inflammation resolved by 2 weeks. Airway fibrosis in ovalbumin-challenged mice that inhaled MWCNT was accompanied by significant increases in two profibrogenic growth factors, PDGF-AA and TGF-β1. Ovalbumin alone induced only TGF-β1, whereas MWCNT alone only induced PDGF-AA. PDGF is the most potent fibroblast mitogen discovered to date and is important in expanding the lung population of fibroblasts (21). TGF-β1 is the primary growth factor that stimulates fibroblasts to produce collagen, which defines fibrotic lesions (22). Together, these two polypeptide growth factors orchestrate a fibrogenic response. While our study suggests potential roles for PDGF and TGF-β1, further work is needed to identify more definitive roles for these mediators in MWCNT-induced airway fibrosis using strategies such as RNAi, small molecule inhibitors, or neutralizing antibodies to knock-down or block the activity of these growth factors or their receptors *in vivo*.

IL-13 is a well-known mediator of allergic asthma and was increased in the lavage fluid of ovalbumin-sensitized mice and also in ovalbumin-challenged mice that received MWCNT exposure. IL-13 has been reported to stimulate lung fibrosis by increasing TGF-β1 production and activating the release of active TGF-β1 from its latent complex (14). Consistent with this report, we observed elevated TGF-β1 protein in the BAL fluid of ovalbumin-challenged mice. We did not observe a significant increase in PDGF-AA in the BAL fluid from ovalbumin-challenged mice, although we have previously reported that IL-13 stimulates the mitogenesis of human lung fibroblasts through a PDGF-AA autocrine loop (13). We have also observed by immunohistochemistry that PDGF-AA and PDGF-CC are increased in the airway epithelium of mice after ovalbumin challenge (unpublished observation). It is possible

that PDGF-AA in ovalbumin-challenged mice is not secreted by the airway epithelium in detectable amounts, although we clearly observed increased PDGF-AA in the BAL fluid of MWCNT-treated mice. IL-13, TGF-β1, and PDGF-AA are all elevated in human asthma, and play important roles in cell signaling pathways that mediate airway fibrosis (23, 24). MWCNT could have their most significant effect in potentiating the effects of allergen challenge by elevating PDGF.

IL-5 mRNA was increased only in mice that received both ovalbumin challenge and MWCNT inhalation. We did not measure IL-5 protein levels due to the limited amount of BAL fluid that was exhausted in ELISAs for IL-13, PDGF-AA, and TGF-β1. Previous studies have shown a modulatory role for IL-5 in promoting pulmonary fibrosis in different animal models (23) and clinical studies indicate a similar effect in humans (25). In the mouse ovalbumin model in particular, neutralization of IL-5 with monoclonal antibodies before multiple pulmonary challenges with ovalbumin decreases peribronchiolar fibrosis (26). Based on these published reports, there is compelling evidence that IL-5 plays a role in airway fibrosis in asthma. It is therefore conceivable that IL-5, which is synergistically increased by the combination of ovalbumin and MWCNT, could play a significant role in mediating the effect of MWCNT toward potentiating airway fibrosis in allergic inflammation.

The calculated dose of MWCNT aerosol we used was an estimate of the dose used in earlier studies that employed the intratracheal instillation method for CNT delivery and which resulted in significant pulmonary fibrosis and granuloma formation (3–7). Also, unlike instillation studies, the majority of MWCNT observed by light microscopy after inhalation were contained within alveolar macrophages, which is not surprising since macrophages avidly engulf inhaled particles and the (2-μm) size of the aggregated MWCNT aerosol was in the range for phagocytic uptake. Also, unlike intratracheal instillation studies (5, 7), histopathology of lungs in the present study showed no evidence of MWCNT agglomerates obstructing the conducting airways or the alveolar region. However, TEM showed that small aggregates of MWCNT or individual nanotubes were present on or beneath the epithelial cell surface throughout the lung.

The increased MCP-1 message expression from the lung tissue of MWCNT-treated mice could play a role in the recruitment of macrophages to sites of MWCNT deposition. The result that inhaled MWCNT agglomerates were almost completely localized in macrophages is consistent with a recent MWCNT inhalation study (10). We previously reported that SWCNT delivered to the lungs of rats by intratracheal instillation stimulate a strong macrophage phagocytic response (6). In that study, we described "carbon bridges," which are bundles of SWCNT connecting two macrophages (6). The frequency of carbon bridge formation induced by SWCNT was relatively low (< 5% of total macrophages), but provided a reliable biomarker of exposure. No such structures were found in the present study using MWCNT. This is perhaps because MWCNT are 30 to 50 nm in width, whereas SWCNT are only 1 to 3 nm in width; approximately the same width as actin filaments that compose the cytoskeleton. Effective sequestration of MWCNT agglomerates may explain why little inflammation or fibrosis was present by 14 days for unsensitized animals, since inflammation and fibrosis in response to MWCNT have previously been reported around sites where large agglomerates deposited and persisted after intratracheal instillation (9). We observed many small aggregates and individual MWCNT by TEM after inhalation. Well-dispersed SWCNT have been reported to cause interstitial fibrosis in the lungs of mice when delivered by intratracheal instillation (4, 8). However, while our inhalation study resulted in well-dispersed MWCNT as determined by light microscopy and TEM evaluation, we did not observe a significant fibrogenic effect in the absence of preexisting inflammation.

Ovalbumin sensitization by intraperitoneal injection followed by intranasal challenge creates a proinflammatory environment in the lung. Particulate pollutants have been reported to increase allergen-induced inflammation and lung function (17, 27, 28). In particular, carbon nanoparticles can aggravate ovalbumin-induced airway inflammation and immunoglobulin production, which is more prominent with smaller particles (27). In that study, the carbon nanoparticles caused airway inflammation but not fibrosis, which is consistent with our previous observation that carbon nanoparticles do not cause lung fibrotic reactions (6). The present study is the first, to our knowledge, to show that a particulate pollutant of any kind can increase airway fibrosis in allergen-challenged mice. The fibrotic response that we observed with MWCNT and ovalbumin was confined to the bronchioles and did not extend into the interstitium, which differs from previous reports showing interstitial fibrosis at sites distant from the airways of unsensitized mice in response to SWCNT (4, 8). Although quantitative morphometry revealed a statistically significant increase in peribronchiolar fibrosis in sensitized animals that inhaled MWCNT, no significant increases in total lung collagen content were observed, which is consistent with our observation of a localized airway response. Moreover, the animals showed no signs of respiratory distress. However, we did not perform pulmonary function tests on mice as has been described previously (19). Therefore, it is unknown whether the increased airway fibrosis in ovalbumin-challenged mice that inhaled MWCNT correlates with decreased lung function. This is an important issue that should be addressed in future investigations. It is also unknown whether the airway fibrotic lesions observed in mice that received a combination of allergen and MWCNT will eventually resolve or progress. Further work should include a longer time course evaluation to address this issue.

In the present study we used an aerosol concentration of approximately 100 mg/m^3 MWCNT and a single exposure 6 hours in duration on a nose-only tower. This dose is admittedly high, but was specifically chosen to fall within the dosing range of MWCNT (0.5–20 mg/kg) delivered to mice by intratracheal instillation (7) or to approximate a dose of SWCNT that we used previously administered to rats by intratracheal instillation. This type of comparison is the only way to directly assess the issue of whether inhalation exposure results in pathology similar to that of intratracheal instillation or pharyngeal aspiration. Moreover, the dose of MWCNT that we used in this study is roughly within the range of previous whole-body inhalation studies that were 0.2–2.7 mg/kg (10) and 2–10.5 mg/kg (9). We estimated an alveolar deposition dose of 12 mg/kg and a tracheobronchial dose of 4 mg/kg for an aerosol of average mass median aerodynamic diameter of approximately 700 nm. Although the airborne concentration of MWCNT in the present study is similar to those at the higher end of the dosing ranges in other MWCNT inhalation studies, it is 2,000-fold greater than the average, estimated concentration of 0.053 mg/m^3 generated during the handling of SWCNT in occupational exposure scenarios (29) and 20-fold greater than the 5 mg/m^3 NIOSH occupational exposure standard for unregulated particulates (30).

The MWCNT used in this study were purchased from a commercial source and characterization provided by the manufacturer and verified by an independent contract laboratory. TEM of the bulk material verified that these were nanotubes, not carbon nanofibers (31, 32), and that MWCNT were aggregated. TGA analysis from both sources were in agreement that bulk MWCNT were greater than 94% in purity. BET surface area was also consistent with an average of 109.29 m^2/g. The elemental

composition of the bulk material was carbon > oxygen > nickel > lanthanum. It is important to note that Ni and La values measured by ICP-AES, in which the nanotubes are treated with strong acid, reflects dissolved surface metals. This measurement is probably more reasonable than EDX measurements for discerning bioavailable metals, since EDX also measures metals embedded within MWCNT. The metal concentrations as a percentage of the bulk material as determined by ICP-AES are low, at 0.34% (Ni) and 0.03% (La). The MWCNT aerosol was also characterized. TEM of the aerosol revealed that MWCNT were mostly agglomerates of approximately 2 μm in size with protruding nanotubes. Agglomeration is likely due to Van der Waals forces between MWCNT (1) that were not disrupted by the Pluronic F-68 surfactant.

A caveat for the present study is that the high dose of MWCNT and the brief duration of exposure do not likely mimic occupational exposure scenarios, which will probably occur with airborne concentrations in the 0.05–5 mg/m^3 range for up to 40 hours per week in duration over weeks to months to years. However, very high airborne concentrations and brief exposures are consistent with the use of inhalants in medicine, and MWCNT are proposed for use in drug delivery applications (33). The result that no acute observable pulmonary hazard of airway fibrosis to normal lung tissue was observed is of importance, especially at the high dose that we used, since the data indicate that the NOAEL for inhaled MWCNT is probably greater than what may be achievable in "real life" occupational or therapeutic exposures. Our data do indicate a pulmonary hazard of increased airway fibrosis in inflamed lung tissue, but the degree of fibrosis was not sufficient to cause overt signs of pulmonary distress. This result supports our original hypothesis, which was that MWCNT cause greater lung injury and fibrosis under conditions of pre-existing allergic inflammation, indicating that individuals with asthma may be more susceptible to adverse effects from MWCNT than normal populations. This study should encourage future investigations into differences in dose–response-effect relationships in normal and asthmatic lung in response to inhaled CNT at airborne concentrations relevant to occupational and medical exposures.

Conflict of Interest Statement: B.A.W. received $25,000 in 2006 and 2007 from the American Chemistry Council's Long Range Research Institute as research funding related to nanoparticle toxicity. None of the other authors has a financial relationship with a commercial entity that has an interest in the subject of this manuscript.

Acknowledgments: The authors thank David Weil, Delorise Williams, Otis Light, Duncan Wallace, Vickie Wong, Elise Barber, and Carol Bobbitt for excellent technical assistance and Joseph Lopez for attentive animal care. Special thanks to Jeanette Shipley-Phillips at NCSU for performing TEM to detect MWCNT in lung. The authors also thank Greg Parsons and Joe Spagnola at NCSU for helpful comments about MWCNT TEM and SEM data, and Ram Bhat at Millenium Research, Inc., for directing contracted MWCNT characterizations.

References

1. Donaldson K, Aitken R, Tran L, Stone V, Duffin R, Forrest G, Alexander A. Carbon nanotubes: a review of their properties in relation to pulmonary toxicology and workplace safety. *Toxicol Sci* 2006;92:5–22.
2. Poland CA, Duffin R, Kinloch I, Maynard A, Wallace WAH, Seaton A, Stone V, Brown S, MacNee W, Donaldson K. Carbon nanotubes introduced into the abdominal cavity of mice show asbestos-like pathogenicity in a pilot study. *Nat Nanotech* 2008;3:423–428.
3. Lam CW, James JT, McCluskey R, Hunter RL. Pulmonary toxicity of single-wall carbon nanotubes in mice 7 and 90 days after intratracheal instillation. *Toxicol Sci* 2004;77:126–134.
4. Shvedova AA, Kisin ER, Mercer R, Murray AR, Johnson VJ, Potapovich AI, Tyurina YY, Gorelik O, Arepalli S, Schwegler-Berry D, *et al.* Unusual inflammatory and fibrogenic pulmonary responses to single-walled carbon nanotubes in mice. *Am J Physiol Lung Cell Mol Physiol* 2005;289:L698–L708.
5. Warheit DB, Laurence BR, Reed KL, Roach DH, Reynolds GA, Webb TR. Comparative pulmonary toxicity assessment of single-wall carbon nanotubes in rats. *Toxicol Sci* 2004;77:117–125.
6. Mangum JB, Turpin EA, Antao-Menezes A, Cesta MF, Bermudez E, Bonner JC. Single-walled carbon nanotube (SWCNT)-induced interstitial fibrosis in the lungs of rats is associated with increased levels of PDGF mRNA and the formation of unique intercellular carbon structures that bridge alveolar macrophages in situ. *Part Fibre Toxicol* 2006;3:15.
7. Muller J, Huaux F, Moreau N, Misson P, Heilier JF, Delos M, Arras M, Fonseca A, Nagy JB, Lison D. Respiratory toxicity of multi-wall carbon nanotubes. *Toxicol Appl Pharmacol* 2005;207:221–231.
8. Mercer RR, Scabilloni J, Wang L, Kisin E, Murray AR, Schwegler-Berry D, Shvedova AA, Castranova V. Alteration of deposition pattern and pulmonary response as a result of improved dispersion of aspirated single-walled carbon nanotubes in a mouse model. *Am J Physiol Lung Cell Mol Physiol* 2008;294:L87–L97.
9. Li JG, Li WX, Xu JY, Cai XQ, Liu RL, Li YJ, Zhao QF, Li QN. Comparative study of pathological lesions induced by multiwalled carbon nanotubes in lungs of mice by intratracheal instillation and inhalation. *Environ Toxicol* 2007;22:415–421.
10. Mitchell LA, Gao J, Wal RV, Gigliotti A, Burchiel SW, McDonald JD. Pulmonary and systemic immune response to inhaled multiwalled carbon nanotubes. *Toxicol Sci* 2007;100:203–214.
11. Brewster CE, Howarth PH, Djukanovic R, Wilson J, Holgate SJ, Roche WR. Myofibroblasts and subepithelial fibrosis in bronchial asthma. *Am J Respir Cell Mol Biol* 1990;3:507–511.
12. Wills-Karp M, Luyimbazi J, Xu X, Schofield B, Neben TY, Karp CL, Donaldson DD. Interleukin-13: central mediator of allergic asthma. *Science* 1998;282:2258–2261.
13. Ingram JL, Antao-Menezes A, Mangum JB, Lyght O, Lee PJ, Elias JA, Bonner JC. Opposing actions of Stat1 and Stat6 on IL-13-induced up-regulation of early growth response-1 and platelet-derived growth factor ligands in pulmonary fibroblasts. *J Immunol* 2006;177:4141–4148.
14. Lee CG, Homer RJ, Zhu Z, Lanone S, Wang X, Koteliansky V, Shipley JM, Gotwals P, Noble P, Chen Q, *et al.* Interleukin-13 induces tissue fibrosis by selectively stimulating and activating transforming growth factor beta(1). *J Exp Med* 2001;194:809–821.
15. Gavett SH, Koren HS. The role of particulate matter in exacerbation of atopic asthma. *Int Arch Allergy Immunol* 2001;124:109–112.
16. Peters A, Wichmann HE, Tuch T, Heinrich J, Heyder J. Respiratory effects are associated with the number of ultrafine particles. *Am J Respir Crit Care Med* 1997;155:1376–1383.
17. Matsumoto A, Hiramatsu K, Li Y, Azuma A, Kudoh S, Takizawa H, Sugawara I. Repeated exposure to low-dose diesel exhaust after allergen challenge exaggerates asthmatic responses in mice. *Clin Immunol* 2006;121:227–235.
18. Miller FJ. Dosimetry of particles in laboratory animals and humans in relationship to issues surrounding lung overload and human health risk assessment: a critical review. *Inhal Toxicol* 2000;12:19–57.
19. Card JW, Voltz JW, Carey MA, Bradbury JA, Degraff LM, Lih FB, Bonner JC, Morgan DL, Flake GP, Zeldin DC. Cyclooxygenase-2 deficiency exacerbates bleomycin-induced lung dysfunction but not fibrosis. *Am J Respir Cell Mol Biol* 2007;37:300–308.
20. Voltz JW, Card JW, Carey MA, Degraff LM, Ferguson CD, Flake GP, Bonner JC, Korach KS, Zeldin DC. Male Sex Hormones Exacerbate Lung Function Impairment After Bleomycin-Induced Pulmonary Fibrosis. *Am J Respir Cell Mol Biol* 2008;39:45–52.
21. Bonner JC. Regulation of PDGF and its receptors in fibrotic diseases. *Cytokine Growth Factor Rev* 2004;15:255–273.
22. Wynn T. Cellular and molecular mechanisms of fibrosis. *J Pathol* 2008; 214:199–210.
23. Doherty T, Broide D. Cytokines and growth factors in airway remodeling in asthma. *Curr Opin Immunol* 2007;19:676–680.
24. Lewis CC, Chu HW, Westcott JY, Tucker A, Langmack EL, Sutherland ER, Kraft M. Airway fibroblasts exhibit a synthetic phenotype in severe asthma. *J Allergy Clin Immunol* 2005;115:534–540.
25. Flood-Page P, Menzies-Gow A, Phipps S, Ying S, Wanoo A, Ludwig MS, Barnes N, Robinson D, Kay BA. Anti-IL-5 treatement reduces deposition of ECM proteins in the nronchial subepithelial basement membrane of mild atopic asthmatics. *J Clin Invest* 2003;112:1029–1036.
26. Cho JY, Miller M, Baek KJ, Han JW, Nayar J, Lee SY, McElwain K, McElwain S, Friedman S, Broide DH. Inhibition of airway remodeling in IL-5-deficient mice. *J Clin Invest* 2004;113:551–560.

27. Inoue K, Takano H, Yanagisawa R, Sakurai M, Ichinose T, Sadakane K, Yoshikawa T. Effects of nano particles on antigen-related airway inflammation in mice. *Respir Res* 2005;6:106.
28. Samuelsen M, Nygaard UC, Lovik M. Allergy adjuvant effect of particles from wood smoke and road traffic. *Toxicology* 2008;246: 124–131.
29. Maynard AD, Baron PA, Foley M, Shvedova AA, Kisin ER, Castranova V. Exposure to carbon nanotube material: aerosol release during the handling of unrefined single-walled carbon nanotube material. *J Toxicol Environ Health A* 2004;67:87–107.
30. NIOSH. Particulates not otherwise regulated. NIOSH Pocket Guide to Chemical Hazards. 2005.
31. Lison D, Muller J. Lung and systemic responses to carbon nanotubes (CNT) in mice. *Toxicol Sci* 2008;101:179–180.
32. Melechko AV, Merkoluv VI, McKnight TE, Guillom MA, Klien KL, Lowndes DH, Simpson ML. Vertically aligned carbon nanofibers and related structures: controlled synthesis and directed assembly. *J Appl Phys* 2005;97:1–39.
33. Bianco A, Kostarelos K, Prato M. Applications of carbon nanotubes in drug delivery. *Curr Opin Chem Biol* 2005;9:674–679.